Numerical Method for Solving the RHGD Equations with MUSCL-Hancock and Cell Centered Diffusion

Zachary Hardy

November 2, 2019

1 Introduction

In this report the radiation-hydrodynamics equations with grey diffusion (RHGD), correct to $\mathcal{O}(u/c)$ are considered. This system is given by the Euler equations of hydrodynamics and the grey diffusion equation for radiation energy density. The grey diffusion is coupled to the Euler equations through a radiation-material momentum deposition term, a radiation-material energy momentum deposition term, and a material-radiation emission term. The equations are given as follows

$$\frac{\partial \rho}{\partial t} + \vec{\nabla} \cdot (\rho \vec{u}) = 0 \tag{1}$$

$$\frac{\partial}{\partial t}(\rho \vec{u}) + \vec{\nabla} \cdot (\rho \vec{u} \otimes \vec{u}) + \vec{\nabla} p = -\frac{1}{3}\vec{\nabla}\mathcal{E} \tag{2}$$

$$\frac{\partial E_m}{\partial t} + \vec{\nabla} \cdot [(E_m + p)\, u] = \rho \kappa_a c \left(\mathcal{E} - aT^4\right) - \frac{1}{3}\vec{u} \cdot \vec{\nabla}\mathcal{E} \tag{3}$$

$$\frac{\partial \mathcal{E}}{\partial t} - \vec{\nabla} \cdot \left(\frac{c}{3\rho\kappa_t}\vec{\nabla}\mathcal{E}\right) + \frac{4}{3}\vec{\nabla} \cdot (\mathcal{E} u) = \rho \kappa_a c \left(aT^4 - \mathcal{E}\right) + \frac{1}{3}\vec{u} \cdot \vec{\nabla}\mathcal{E} \quad , \tag{4}$$

where,

$$E_m = \rho \left(\frac{1}{2}u^2 + e\right) \tag{5}$$

$$p = (\gamma - 1)\, \rho e \tag{6}$$

$$T = \frac{e}{C_v} \quad . \tag{7}$$

For this application, it will be assumed that the opacities, κ, are functions of temperature, and that the specific heat, C_v is a constant.

The discretization discussed in this report will be in the Eulerian frame. It will use the MUSCL-Hancock scheme for the Euler equations with an HLLC Riemann solver [1] [2] [5],

cell-centered diffusion for the radiation energy density equation, and a double minmod slope limiter for stabalization [3]. This particular slope limiter is used because in McClarren et. al., it was shown that this slope limiter is asymptotic-preserving. Operator splitting will be employed such that the MUSCL-Hancock method for the homogeneous Euler equations is still applicable and to separate the advection-diffusion-reaction radiation energy density equation into a purely advective problem, and a diffusion-reaction problem. This will result in the existence of intermittent states of the unknown variables. These states will arise when only part of one of the equations above have been solved. All intermittent states will be denoted with the time-step index for which the intermittent state is advancing towards, and a * to indicate that it is an intermittent state. For example, an intermittent state of variable U advancing towards the value of U at t^n is given by $U^{n,*}$.

The numbering of cells in space will follow that of cell-centered diffusion. Cell edges will be denoted with half integer indices, and cell centers with integer indices. For instance, for cell i, the left (inner) edge, center, and right (outer) edge are denoted $i-\frac{1}{2}$, i , and $i+\frac{1}{2}$, respectively. This same notation is used for the temporal cells, where the beginning, middle, and end of a time-step have indices of $n-\frac{1}{2}$, n , and $n+\frac{1}{2}$, respectively.

This method will take the form of a predictor-corrector scheme, use an implicit-explicit (IMEX) discretization in time. More specifically, the mass, momentum, and kinetic energy terms will be treated explicitly, while the specific material internal energy and radiation energy terms will be treated using Crank-Nicholson in time. This report is written for a generalized geometry, which leads to the following standard cell volume and cell edge area definitions

$$V_i = r_{i+\frac{1}{2}} - r_{i-\frac{1}{2}} \qquad \text{(planar)} \tag{8}$$

$$= \pi\left(r^2_{i+\frac{1}{2}} - r^2_{i-\frac{1}{2}}\right) \qquad \text{(cylindrical)} \tag{9}$$

$$= \frac{4}{3}\pi\left(r^3_{i+\frac{1}{2}} - r^3_{i-\frac{1}{2}}\right) \qquad \text{(spherical)} \ , \tag{10}$$

and,

$$A_{i+\frac{1}{2}} = 1 \qquad \text{(planar)} \tag{11}$$

$$= 2\pi r_{i+\frac{1}{2}} \qquad \text{(cylindrical)} \tag{12}$$

$$= 4\pi r^2_{i+\frac{1}{2}} \qquad \text{(spherical)} \ . \tag{13}$$

The remainder of this report will outline the numerical algorith, discuss the handling of boundary conditions, and then present the results of a steady state planar radiative shock problem.

2 Numerical Algorithm

Predictor

1) **Generate Slopes and Edge Values for Hydrodynamic Variables**
The first step in this algorithm is to generate a linear discontinuous representation of the conserved hydrodynamic variables, mass, momentum, and material energy densities. This is done by generating cell averaged slopes (differences) and corresponding edge values for each cell. First, the differences in the conserved variables are generated using the cell centered values at $t^{n-\frac{1}{2}}$ via

$$\Delta_{i+\frac{1}{2}} = U_{i+1} - U_i \quad , \quad i = 1, N-1 \tag{14}$$

$$\Delta_{i-\frac{1}{2}} = U_i - U_{i-1} \quad , \quad i = 2, N \quad , \tag{15}$$

where U is any of the conserved hydrodynamic quantities. The slopes are then computed using a weighted average

$$\Delta_i = \frac{1}{2}(1+\omega)\Delta_{i-\frac{1}{2}} + \frac{1}{2}(1-\omega)\Delta_{i+\frac{1}{2}} \quad , \tag{16}$$

where, $\omega = 0$.

Now, the slopes are limited such that

$$\bar{\Delta}_i = \xi_i \Delta_i \quad , \tag{17}$$

where ξ_i is obtained using a slope limiter of the users choice that satisfies the conditions of TVD. The edge values of the hydrodynamic variables at $t^{n-\frac{1}{2}}$ are given by

$$U_{i,L} = U_i - \frac{1}{2}\bar{\Delta}_i \quad , \quad i = 2, N \tag{18}$$

$$U_{i,R} = U_i + \frac{1}{2}\bar{\Delta}_i \quad , \quad i = 1, N-1 \quad . \tag{19}$$

In addition to this, edge pressures, $p^{n-\frac{1}{2}}_{i,L(R)}$ are defined using Eq. (6). These edge values are later used to compute edge fluxes for the predictor step of the MUSCL-Hancock method.

2) **Generate Slopes and Edge Values for the Radiation Energy Density**
Using the same formulas as above, limited slopes and edge values for the radiation energy density are computed. This results in the following evaluated at $t^{n-\frac{1}{2}}$

$$\mathcal{E}_{i,L} = \mathcal{E}_i - \frac{1}{2}\bar{\Delta}_i \quad , \quad i = 2, N \tag{20}$$

$$\mathcal{E}_{i,R} = \mathcal{E}_i + \frac{1}{2}\bar{\Delta}_i \quad , \quad i = 1, N-1 \quad , \tag{21}$$

where $\bar{\Delta}_i$'s are defined equivalently to those of the previous step. These are later used to compute radiation energy edge fluxes which are used to obtain the advection contributions to $\mathcal{E}$.

3) **Evolve Hydrodynamic Variables a Half Time Step**
This step is the predictor step of the MUSCL-Hancock method for the homogeneous Euler equations, Eq. (1) - Eq. (3) without radiation sources. Here, the hydrodynamic variables are evolved a half time step. In the MUSCL-Hancock method, the edge values are evolved because those values can then be used in the Riemann solver, however, because the radiation contributions still must be accounted for, the center values are evolved for compatibility with the radiation energy density equation. It should be noted that in the MUSCL-Hancock method the edge values are evolved identically (i.e. the slope does not change), and therefore, evolving the center value is equivalent to evolving an edge value and then recomputing the center value using the computed slopes. The discrete equations are formed by integrating the homogeneous Euler equations over the volume of cell i and over the half time step interval $\Delta t^n/2$. The fluxes are evaluated using the previously computed edge values at $t^{n-\frac{1}{2}}$, resulting in the following equation for the intermittent state of the hydrodynamic variables at t^n

$$U_i^{n,*} = U_i^{n-\frac{1}{2}} + \frac{\Delta t^n}{2V_i}\left(A_{i-\frac{1}{2}}F(U_{i,L}^{n-\frac{1}{2}}) - A_{i+\frac{1}{2}}F(U_{i,R}^{n-\frac{1}{2}})\right) \tag{22}$$

where,

$$U = \begin{pmatrix} \rho \\ \rho u \\ E_m \end{pmatrix} \quad , \quad F(U) = \begin{pmatrix} \rho u \\ \rho u^2 + p \\ (E_m + p)u \end{pmatrix} \quad . \tag{23}$$

It should be noted that this step gives the final predicted mass density at t^n, ρ^n, because there is no coupling between the radiation energy density equation and the mass density equation, thus, all effects on density are considered in this step. Implicitly, each of the primitive variables intermittent states, $u^{n,*}$, $e^{n,*}$, $P^{n,*}$, and $T^{n,*}$ are known at this point as well.

4) **Advect the Radiation Energy Density a Half Time Step**
The purely hyperbolic portion of the radiation energy density equation is now solved. This is advantageous because it separates the advection-diffusion-reaction radiation energy density problem into an advection problem and a diffusion-reaction problem, both of which have well defined discretization methods which can be applied. The purely advective radiation energy density problem is

$$\frac{\partial \mathcal{E}}{\partial t} + \frac{4}{3}\vec{\nabla}\cdot(\mathcal{E}u) = 0 \quad . \tag{24}$$

The discrete equations are obtained identically to those in the previous step

$$\mathcal{E}_i^{n,*} = \mathcal{E}_i^{n-\frac{1}{2}} + \frac{4}{3}\frac{\Delta t^n}{2V_i}\left(A_{i-\frac{1}{2}}\left(\mathcal{E}u\right)_{i,L}^{n-\frac{1}{2}} - A_{i+\frac{1}{2}}\left(\mathcal{E}u\right)_{i,R}^{n-\frac{1}{2}}\right) \quad , \tag{25}$$

where $\mathcal{E}^{n-\frac{1}{2}}_{i,L(R)}$ was previously computed, and $u^{n-\frac{1}{2}}_{i,L(R)}$ is derived via the edge values of the conserved hydrodynamic variables

$$u^{n-\frac{1}{2}}_{i,L(R)} = \frac{(\rho u)^{n-\frac{1}{2}}_{i,L(R)}}{\rho^{n-\frac{1}{2}}_{i,L(R)}} \tag{26}$$

This yields an intermittent state for the half time step value of the radiation energy density, $\mathcal{E}^{n,*}$. In the next steps, the radiation-material momentum and energy deposition and material-radiation emission is considered.

5) **Add Radiation-Material Momentum Deposition**
The material momentum deposition from the radiation field is now considered. In differential form

$$\frac{\partial}{\partial t}(\rho u) = -\frac{1}{3}\vec{\nabla}\mathcal{E} \quad . \tag{27}$$

Integrating this over a half time step and cell volume, the discrete equation for cell i

$$M^n_i = M^{n,*}_i - \frac{1}{3}\frac{\Delta t^n}{2V_i}\left(A_{i+\frac{1}{2}}\mathcal{E}^{n-\frac{1}{2}}_{i+\frac{1}{2}} - A_{i-\frac{1}{2}}\mathcal{E}^{n-\frac{1}{2}}_{i-\frac{1}{2}}\right) \quad , \tag{28}$$

where M is the material momentum, and $\mathcal{E}_{i\pm\frac{1}{2}}$ is obtained by enforcing continuity of radiation energy density current at each cell interface, respectively. This turns out to be a harmonic mean weighted by the diffusion coefficients divided by cell widths

$$\mathcal{E}_{i+\frac{1}{2}} = \frac{\frac{D_{i+1,i+\frac{1}{2}}}{\Delta r_{i+1}}\mathcal{E}_{i+1} + \frac{D_{i,i+\frac{1}{2}}}{\Delta r_i}\mathcal{E}_i}{\frac{D_{i+1,i+\frac{1}{2}}}{\Delta r_{i+1}} + \frac{D_{i,i+\frac{1}{2}}}{\Delta r_i}} \quad , \tag{29}$$

where,

$$D_{i+1,i+\frac{1}{2}} = \frac{1}{\rho_{i+1}\kappa_{t,i+1,i+\frac{1}{2}}} \quad , \tag{30}$$

$\kappa_{t,i+1,i+\frac{1}{2}}$ is the cell centered opacity evaluated at the edge temperature given by

$$T_{i+\frac{1}{2}} = \left[\left(T^4_{i+1} + T^4_i\right)/2\right]^{1/4} \quad , \tag{31}$$

and all quantities are evaluated at the same time as the edge radiation energy, $t^{n-\frac{1}{2}}$. Solving Eq. (28), the half time step momentum, and therefore, the velocity at t^n is now known.

6) **Add Radiation-Material Energy Deposition**
In this step, the final two unknowns will be solved for, the material internal energy

density and the radiation energy density. Each of these will be treated using Crank-Nicholson in time. Because of this, the radiation energy density and specific internal energy equations must either be solved simultaneously, or by eliminating one of the quantities from one equation and solving them separately. In this algorithm, they will be solved simultaneously. It should be noted that the hydrodynamic effects in the specific internal energy equation have already been considered, therefore, the equations in this step include only coupling terms to the radiation field. In differential form,

$$\frac{\partial}{\partial t}\rho\left(\frac{1}{2}u^2+e\right)=\rho\kappa_a c\left(\mathcal{E}-aT^4\right)-\frac{1}{3}\vec{u}\cdot\vec{\nabla}\mathcal{E} \tag{32}$$

$$\frac{\partial\mathcal{E}}{\partial t}-\vec{\nabla}\cdot\left(\frac{c}{3\rho\kappa_t}\vec{\nabla}\mathcal{E}\right)=\rho\kappa_a c\left(aT^4-\mathcal{E}\right)+\frac{1}{3}\vec{u}\cdot\vec{\nabla}\mathcal{E}\quad . \tag{33}$$

It should be be noted that all kinetic energy deposition terms will be treated explicitly. To handle the non-linear temperature term, a single Newton iteration is used and a change of variable from temperature to specific internal energy is introduced. This done by taking advantage of Eq. (7) as follows

$$\frac{1}{2}\left(T_i^{4,n}+T_i^{4,n-\frac{1}{2}}\right)=\frac{1}{2}\left[\left(T_i^{4,n,*}+4T_i^{3,n,*}\left(T_i^n-T_i^{n,*}\right)\right)+T_i^{4,n-\frac{1}{2}}\right] \tag{34}$$

$$=\frac{1}{2}\left[\left(T_i^{4,n,*}+4T_i^{3,n,*}\frac{e_i^n-e_i^{n,*}}{C_v}\right)+T_i^{4,n-\frac{1}{2}}\right]\quad . \tag{35}$$

The discretized system is obtained again by integrating over cell volumes and a half time step. The radiation energy density and specific internal energy densities will be indexed at $t^{n-\frac{1}{4}}$ to indicate a simple average of that quantity over the time interval $t\in[t^{n-\frac{1}{2}},t^n]$. The discrete system is then

$$\begin{aligned}\frac{2V_i}{\Delta t^n}\rho_i^n\left[\left(\frac{1}{2}u^2+e\right)_i^n-\left(\frac{1}{2}u^2+e\right)_i^{n,*}\right]&=-\frac{1}{3}\left(A_{i+\frac{1}{2}}\mathcal{E}_{i+\frac{1}{2}}^{n-\frac{1}{2}}-A_{i-\frac{1}{2}}\mathcal{E}_{i-\frac{1}{2}}^{n-\frac{1}{2}}\right)u_i^{n-\frac{1}{2}}\\&+V_i\rho_i^n\kappa_{a,i}^{n-\frac{1}{2}}c\left[\mathcal{E}_i^{n-\frac{1}{4}}-\frac{1}{2}a\left(T_i^{4,n-\frac{1}{2}}+T_i^{4,n,*}+4T_i^{3,n,*}\frac{e_i^n-e_i^{n,*}}{C_v}\right)\right]\quad ,\end{aligned} \tag{36}$$

$$\begin{aligned}&\frac{2V_i}{\Delta t^n}\left(\mathcal{E}_i^n-\mathcal{E}_i^{n,*}\right)+A_{i+\frac{1}{2}}\mathcal{F}_{0,i+\frac{1}{2}}^{n-\frac{1}{4}}-A_{i-\frac{1}{2}}\mathcal{F}_{0,i-\frac{1}{2}}^{n-\frac{1}{4}}=\\&\quad V_i\rho_i^n\kappa_{a,i}^{n-\frac{1}{2}}c\left[\frac{1}{2}a\left(T_i^{4,n-\frac{1}{2}}+T_i^{4,n,*}+4T_i^{3,n,*}\frac{e_i^n-e_i^{n,*}}{C_v}\right)-\mathcal{E}_i^{n-\frac{1}{4}}\right]\\&\quad+\frac{1}{3}\left(A_{i+\frac{1}{2}}\mathcal{E}_{i+\frac{1}{2}}^{n-\frac{1}{2}}-A_{i-\frac{1}{2}}\mathcal{E}_{i-\frac{1}{2}}^{n-\frac{1}{2}}\right)u_i^{n-\frac{1}{2}}\quad ,\end{aligned} \tag{37}$$

where $\mathcal{F}_{0,i+\frac{1}{2}}$ is the radiation energy flux in the comoving-frame at cell edge $i+\frac{1}{2}$, given by

$$\mathcal{F}_{0,i+\frac{1}{2}}^{n-\frac{1}{4}} = -\frac{2c\left(\mathcal{E}_{i+1}^{n-\frac{1}{4}} - \mathcal{E}_{i}^{n-\frac{1}{4}}\right)}{3\left(\rho_{i+1}^{n-\frac{1}{4}}\Delta r_{i+1}\kappa_{t,i+1,i+\frac{1}{2}}^{n-\frac{1}{2}} + \rho_{i}^{n-\frac{1}{4}}\Delta r_{i}\kappa_{t,i,i+\frac{1}{2}}^{n-\frac{1}{2}}\right)} \quad , \tag{38}$$

where $\kappa_{t,i,i+\frac{1}{2}}$ is defined similarly to in the previous step.

After simultaneously solving this system for e^n and $\mathcal{E}^n$, and therefore, E_m^n, all predicted values at t^n are implicitly known by using definitions of the conserved hydrodynamic quantities and equations of state.

Corrector

1) **Regenerate Slopes and Edge Values for Hydrodynamic Variables at t^n**
Because the hydrodynamic variable slopes may have been distorted by the effects of the radiation field, they must be regenerated for the predicted hydrodynamic variables at t^n so that the necessary time-centered edge values can be obtained for the approximate Riemann solver. These slopes are generated and limited identically to those in the predictor step, as are the edge values. This is to include the calculation of edge pressures with Eq. (6).

2) **Regenerate Slopes and Edge Values for the Radiation Energy Density**
These slopes are generated identically to those in the predictor step.

3) **Evolve the Hydrodynamic Variables a Full Time Step**
The homogeneous Euler equations are now solved over a full time step. Whereas befor the fluxes were found using the constructed edge values, now, the fluxes are computed using an HLLC Approximate Riemann Solver. Details on this can be found in the MUSCL-Hancock Memo or in Toro's book. Upon integrating the equations over a spatial cell volume and a full time step, the following is obtained for arbitrary hydrodynamic variable U

$$U_i^{n+\frac{1}{2},*} = U_i^{n-\frac{1}{2}} + \frac{\Delta t^n}{V_i}\left(A_{i-\frac{1}{2}}F_{i-\frac{1}{2}}^n - A_{i+\frac{1}{2}}F_{i+\frac{1}{2}}^n\right) \quad , \tag{39}$$

where F is obtained by using the HLLC Approximate Riemann solver. Details on the HLLC Riemann solver will not be discussed here. More information can be found in Toro.

The result of this is the intermittent state of the conserved hydrodynamic variables at $t^{n+\frac{1}{2}}$. In addition, as before, because there is no radiation-mass density coupling, the

mass density obtained here is the final mass density for $t^{n+\frac{1}{2}}$, $\rho^{n+\frac{1}{2}}$. The intermittent values for all hydrodynamic quantities, as in the predictor, are implicitly know from this step.

4) **Advect the Radiation Energy Density a Full Time Step**
Next, the radiation energy density is advected for a full time step using upwinded based on the sign of the velocity component. As before, the velocity is derived from the hydrodynamic edge values via

$$u^n_{i,L(R)} = \frac{(\rho u)^n_{i,L(R)}}{\rho^n_{i,L(R)}} \quad . \tag{40}$$

This leads to the following discrete equation for the advection of the radiation energy density

$$\mathcal{E}_i^{n+\frac{1}{2},*} = \mathcal{E}_i^{n-\frac{1}{2}} + \frac{\Delta t^n}{V_i}\left(A_{i-\frac{1}{2}}\left(\mathcal{E}u\right)^n_{i-\frac{1}{2}} - A_{i+\frac{1}{2}}\left(\mathcal{E}u\right)^n_{i+\frac{1}{2}}\right) \quad , \tag{41}$$

where the fluxes are upwinded according to:

$$\left(\mathcal{E}u\right)^n_{i+\frac{1}{2}} = \begin{cases} \left(\mathcal{E}u\right)^n_{i,R} & , \quad \text{if } u_{i,R},\ u_{i+1,L} > 0 \\ \left(\mathcal{E}u\right)^n_{i+1,L} & , \quad \text{if } u_{i,R}, u_{i+1,L} < 0 \\ \left(\mathcal{E}u\right)^n_{i,R} + \left(\mathcal{E}u\right)^n_{i+1,L} & , \quad \text{if } u_{i+1,L} < 0 < u_{i,R} \\ 0 & , \quad \text{if } u_{i,R} < 0 < u_{i+1,L} \quad . \end{cases} \tag{42}$$

This yields, as before, an intermittent value of the radiation energy density at $t^{n+\frac{1}{2}}$.

5) **Add Radiation-Material Momentum Deposition**
This step is similar to that of the predictor, the only difference being that the radiation-material momentum deposition term is now evaluated at t^n and that a full time step is taken, not a half. This is given as

$$M_i^{n+\frac{1}{2}} = M_i^{n+\frac{1}{2},*} - \frac{1}{3}\frac{\Delta t^n}{V_i}\left(A_{i+\frac{1}{2}}\mathcal{E}^n_{i+\frac{1}{2}} - A_{i-\frac{1}{2}}\mathcal{E}^n_{i-\frac{1}{2}}\right) \quad , \tag{43}$$

where the edge radiation energy densities are found identically to those in the predictor, with continuity of the radiation energy density current. Refer to the radiation-material momentum deposition step of the predictor for more information about this. With this $u^{n+\frac{1}{2}}$ becomes known because $\rho^{n+\frac{1}{2}}$ is known from the hydrodynamics advection step before.

6) **Add Radiation-Material Energy Deposition**
This step is also similar to that of the predictor, the difference being that the radiation-material kinetic energy term is now evaluated with the predicted values

at t^n and that a full time step is taken rather than a half. The radiation energy density and specific internal energy densities are treated with Crank-Nicholson in time as before. In the notation used before, quantities at t^n would now represent the Crank-Nicholson averaged quantities. This coincides with the notation used for the predictor step values. To distinguish between the two, quantities with an index of n will represent the Crank-Nicholson averaged quantities and those designated with an n, p, the predictor quantities. The equations to be simultaneously solved then become

$$\begin{aligned}\frac{V_i}{\Delta t^n}\rho_i^{n+\frac{1}{2}}&\left[\left(\frac{1}{2}u^2+e\right)_i^{n+\frac{1}{2}}-\left(\frac{1}{2}u^2+e\right)_i^{n+\frac{1}{2},*}\right]=-\frac{1}{3}\Bigg(A_{i+\frac{1}{2}}\mathcal{E}_{i+\frac{1}{2}}^{n,p}\\&-A_{i-\frac{1}{2}}\mathcal{E}_{i-\frac{1}{2}}^{n,p}\Bigg)u_i^{n,p}+V_i\rho_i^{n+\frac{1}{2}}\kappa_{a,i}^{n,p}c\Bigg[\mathcal{E}_i^n-\frac{1}{2}a\Bigg(T_i^{4,n-\frac{1}{2}}+T_i^{4,n+\frac{1}{2},*}\\&+4T_i^{3,n+\frac{1}{2},*}\frac{e_i^{n+\frac{1}{2}}-e_i^{n+\frac{1}{2},*}}{C_v}\Bigg)\Bigg]\quad,\end{aligned}\tag{44}$$

$$\begin{aligned}&\frac{V_i}{\Delta t^n}\left(\mathcal{E}_i^{n+\frac{1}{2}}-\mathcal{E}_i^{n+\frac{1}{2},*}\right)+A_{i+\frac{1}{2}}\mathcal{F}_{0,i+\frac{1}{2}}^n-A_{i-\frac{1}{2}}\mathcal{F}_{0,i-\frac{1}{2}}^n=\\&\quad V_i\rho_i^{n+\frac{1}{2}}\kappa_{a,i}^{n,p}c\left[\frac{1}{2}a\left(T_i^{4,n-\frac{1}{2}}+T_i^{4,n+\frac{1}{2},*}+4T_i^{3,n+\frac{1}{2},*}\frac{e_i^{n+\frac{1}{2}}-e_i^{n+\frac{1}{2},*}}{C_v}\right)-\mathcal{E}_i^n\right]\\&\quad+\frac{1}{3}\left(A_{i+\frac{1}{2}}\mathcal{E}_{i+\frac{1}{2}}^{n,p}-A_{i-\frac{1}{2}}\mathcal{E}_{i-\frac{1}{2}}^{n,p}\right)u_i^{n,p}\quad,\end{aligned}\tag{45}$$

where $\mathcal{F}_{0,i+\frac{1}{2}}^n$ is edge comoving-frame radiation energy flux, given by

$$\mathcal{F}_{0,i+\frac{1}{2}}^n=-\frac{2c\left(\mathcal{E}_{i+1}^n-\mathcal{E}_i^n\right)}{4\left(\rho_{i+1}^n\Delta r_{i+1}\kappa_{t,i+1,i+\frac{1}{2}}^{n,p}+\rho_i^n\Delta r_i\kappa_{t,i,i+\frac{1}{2}}^{n,p}\right)}\quad,\tag{46}$$

where $\kappa_{t,i,i+\frac{1}{2}}^{n,p}$ is defined similarly to that of the predictor. Solving this system of equations, the final values of all quantities for the time step are known, as before.

3 Boundary Conditions

For hydrodynamics, there are a few options for boundary conditions, transmissive, fixed, reflective, and periodic. A transmissive boundary condition is set such that the hydrodynamic fluxes on the boundary from the inside and outside are equivalent. This is equivalent

to defining two ficticious ghost cells on the boundary such that

$$\begin{cases} U_0 = U_1, & U_{-1} = U_2 \\ U_{N+1} = U_N, & U_{N+2} = U_{N-1}. \end{cases} \tag{47}$$

It can then be shown that the edge values on either side from either boundary are identical after computing slopes and edge values in the first real and ghost boundary cell normally. This is the preferred boundary condition for shock problems as that it guarantees that waves passing through the boundary are unaffected [5].

Next, there are fixed boundary conditions in which a hydrodynamic state is specified as the boundary value [1]. The outside boundary fluxes are computed using this state. This boundary condition does not have the guarantee of a transmissive boundary condition, but for a steady state shock problem, similar results should be obtained because in general, the slope across the boundary cells will be zero.

A reflective boundary condition is analogous to imposing a fixed wall boundary condition. Again, two ghost cells are on the boundaries. The hydrodynamic states are set similarly to those in a transmissive boundary condition, however, the velocities are defined to be equal and opposite to those in a transsmissive boundary condition. This imposes that no material exits through the boundary and a force given by the edge pressure is exerted on the material at the boundary [5].

Lastly, a periodic boundary condition exists in which the hydrodynamic fluxes on the outside of a boundary edge are given by the hydrodynamic flux on the opposite interior boundary edge such that This can be done by setting one ghost cells on either boundary such that $U_0 = U_N$ and $U_{N+1} = U_0$ to compute slopes in the boundary cells And then using $F_{0,R} = F_{N,R}$ and $F_{N+1,L} = F_{0,L}$ based upon those [1].

For the grey diffusion radiation energy equation, standard boundary conditions are used, either reflective or a incident flux (source). A reflective boundary condition the boundary value of the radiation energy is always set to the cell centered value in the first cell, hence $\mathcal{F}_{0,1/2},\ \mathcal{F}_{0,N+1/2} = 0$, where

$$\mathcal{F}_{0,1/2} = -\frac{2c}{3\rho_1\kappa_{t,1,1/2} + 4}\left(\mathcal{E}_1 - \mathcal{E}_L^b\right), \tag{48}$$

and $\mathcal{F}_{0,N+1/2}$ is defined similarly. A source condition is defined such that

$$\begin{cases} \mathcal{E}_L^b = \mathcal{E}_{1/2} + 2\mathcal{F}_{0,1/2} \\ \mathcal{E}_R^b = \mathcal{E}_{N+1/2} - 2\mathcal{F}_{0,N+1/2}. \end{cases} \tag{49}$$

Reflective boundary conditions are preferred for steady state shock problems, however, source conditions can be used if set to the pre- and post-shock states [4].

4 Time Step Controls

The time step controls used are similar to those given in Bolding et. al., the MUSCL-Hancock memorandum, and Toro [1] [2] [5]. These time-step controls require a user specified CFL condition such that $0 < C_{cfl} < 1$. The time-steps are bounded such that no wave produced from a local Riemann problem can propegate a full cell-width in the predictor step. Because the wave speeds are not known, the cell centered values are used to estimate the sound speeds via

$$S_{max} = \max_i \left(|u_i| + |a_i| \right). \tag{50}$$

The CFL condition is given by

$$C_{cfl} = \frac{S_{max}}{\Delta x / \frac{\Delta t}{2}}. \tag{51}$$

This then yields the following condition for a given time step n,

$$\Delta t_{hydro} = 2 C_{cfl} \min_i \left(\frac{\Delta x}{S^n_{max}} \right). \tag{52}$$

The time step is then given by the minimum of this time step and a user-specified maximum time step

$$\Delta t^n = \min \left(\Delta t_{hydo},\ \Delta t_{max} \right). \tag{53}$$

5 Energy Conservation

On of the simplest ways to perform code verification for this method is to ensure that total energy, that is total material energy plus radiaition energy is conserved. This is done by integrating the sum of the total energy equation and the radiation energy equation over the spatial and temporal domain. Without showing all of the details, this leads to the expression

$$\begin{aligned} 0 = \sum_{i=1}^{N} V_i \left(E^{n+1/2}_{m,i} + \mathcal{E}^{n+1/2}_i - E^{1/2}_{m,i} - \mathcal{E}^{1/2}_i \right) + \\ \sum_{n'=1}^{n} \Big[A_{N+1/2} \left(\mathcal{F}^{n'}_{0,N+1/2} + \left(E^{n',p}_{m,N+1/2} + {}^{n',p}_{N+1/2} \right) u^{n',p}_{N+1/2} \right) \\ - A_{1/2} \left(\mathcal{F}^{n'}_{0,1/2} + \left(E^{n',p}_{m,1/2} + P^{n'p}_{1/2} \right) u^{n',p}_{1/2} \right) \Big] \Delta t^{n'} \end{aligned} \tag{54}$$

6 Code Description

In this section, a brief description of the organization of the program used to execute this algoirthm will be given. This algorithm was programmed in Python using object

oriented programming principles. To simplify the input to the solve the problem, and input parameters class was created to house each of the necessary inputs. In a run file, the user should initialize an input parameters object and define each of the fields to the desired input. With a defined input parameters object, the user passes this to the Eulerian radiation hydrodynamics class to instantiate the problem.

When the problem is instantiated, a number of supporting objects are created. Among these is a geometry class which generates the spatial mesh information, the materials class which houses material properties, equations of state, opacities, etc., and the fields class which holds all of the unknown field variables and many supporting functions. There is also a data reconstruction class which is available for computing slopes, edge values, fluxes, etc., and a Riemann solver class used in the corrector hydrodynamics advection step.

To handle the physics within the problem, each of the steps of the algorithm have their own designated class. For instance, there is a class for hydrodynamics advection, radiation advection, momentum coupling, and energy coupling. Within each class there is a method which carries out the solve of the respective physics in either the predictor or corrector step and updates the correct field variables in the fields class. For more information about the code, see the documented source code.

7 Planar Radiative Shock Problem Results

This section will discuss the results for a steady state planar radiative shock problem with mach 1.2 and mach 3 shocks. The specific heat and thermodynamic constant, C_v and γ, respectively, are constant, the absorption opacity is a function of temperature, given by $\kappa_a(T) = \kappa_1/(\kappa_2 T^n + \kappa_3)$, where κ_i for $i = 1, 2, 3$ and n are constants, and the scattering opacity is zero. Table 1 defines these parameters, the fundamental physical constants a and c, and the domain information

Table 1: Physical constants.

Quantity (units)	Value
C_v $(jerks/cm^3 - keV)$	0.14472799784454
γ (cm^3/g)	5/3
$[\kappa_1, \kappa_2, \kappa_3, n]$	[577.35, 0, 1, 0]
κ_s (cm^2/g)	0
a $(jerks/cm^3 - keV^4)$	0.01372
c (cm/sh)	299.792
R_L (cm)	-0.25
R_R (cm)	0.25
$T_{final}(sh)$	1.5

The pre- and post-shock states for the mach 1.2 shock are given in Table **??**. The

Table 2: Pre- and post-shock states for a mach 1.2 radiative shock.

Quantity (units)	Pre-Shock	Post-Shock
ρ (g/cm^3)	1.0	1.29731782
u (cm/sh)	0.152172533	0.117297805
T (keV)	0.1	0.119475741
$\mathcal{E}$ $(jerks/cm^3)$	1.37201720e-6	2.79562228e-6

simulation was run with 1000 spatial cells using the time step control criteria presented above with a maximum time step of 0.01 sh. The steady state radiative shock solution is given in Figure 1

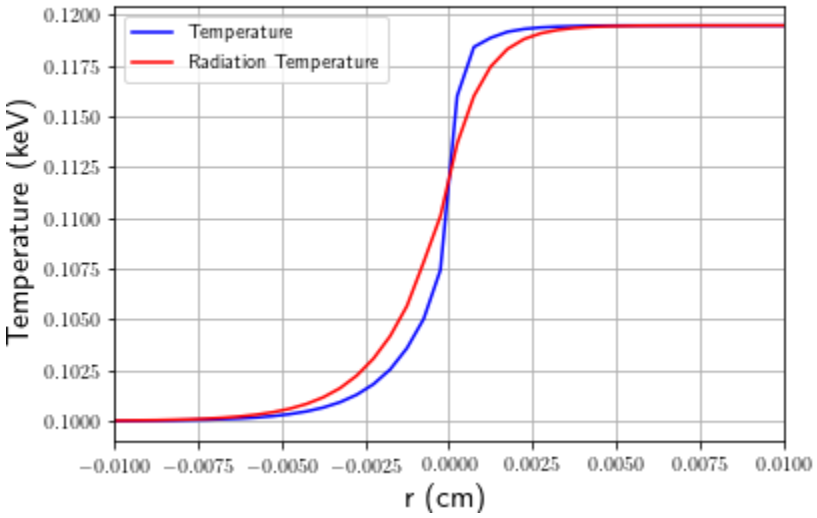

Figure 1: Steady state mach 1.2 radiative shock solution.

The pre- and post-shock states for the mach 3 shock are given in Table 3. The simulation

Table 3: Pre- and post-shock states for a mach 3 radiative shock.

Quantity (units)	Pre-Shock	Post-Shock
ρ (g/cm^3)	1.0	3.00185103
u (cm/sh)	0.380431331	0.126732249
T (keV)	0.1	0.366260705
$\mathcal{E}$ $(jerks/cm^3)$	1.37201720e-6	2.46899872e-4

was run with 2500 spatial cells using the time step control criteria presented above with a

maximum time step of 0.001 sh and a CFL factor of 0.3. The steady state radiative shock solution is given in Figure 2.

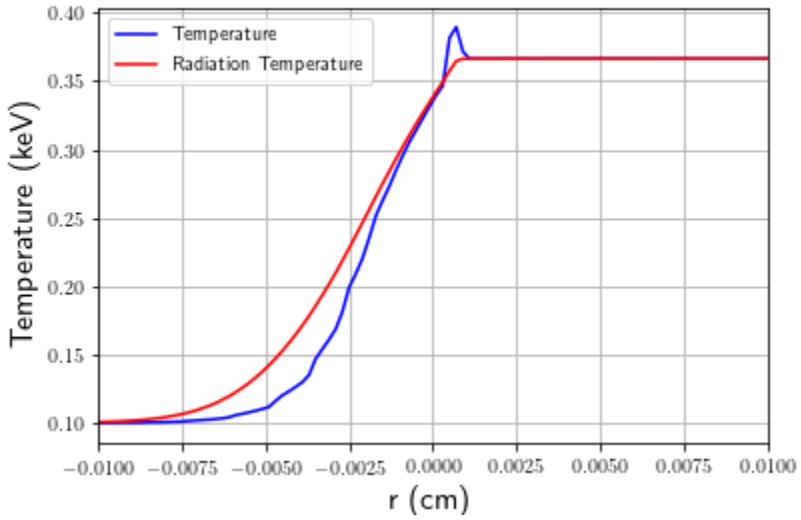

Figure 2: Steady state mach 3 radiative shock solution.

8 Hydrodynamics Shock Tube Problem Results

As a verification for time-dependent problems, the hydrodynamics shock tube problem is tested. In this problem, the initial condition is set to be two distinct hydrodynamic states with zero velocity, kept separate by a membrane. At the start of the simulation, the membrane is broken and the states begin to mix. This produces a left rarefaction wave, a contact wave, and a right shock. The states are given in terms of density, velocity, and pressure are shown in Table 4. In this problem the domain is $x \in [-0.5, 0.5]$ cm and the

Table 4: Left and right states for the shock tube problem.

Quantity (units)	Left-State	Right-State
ρ (g/cm^3)	1.0	0.125
u (cm/sh)	0	0
P (keV)	1.0	0.1

final time is 0.2 sh. The CFL factor is set to 0.5 and the maximum time step to 0.001 sh. The results are shown in Figure 3.

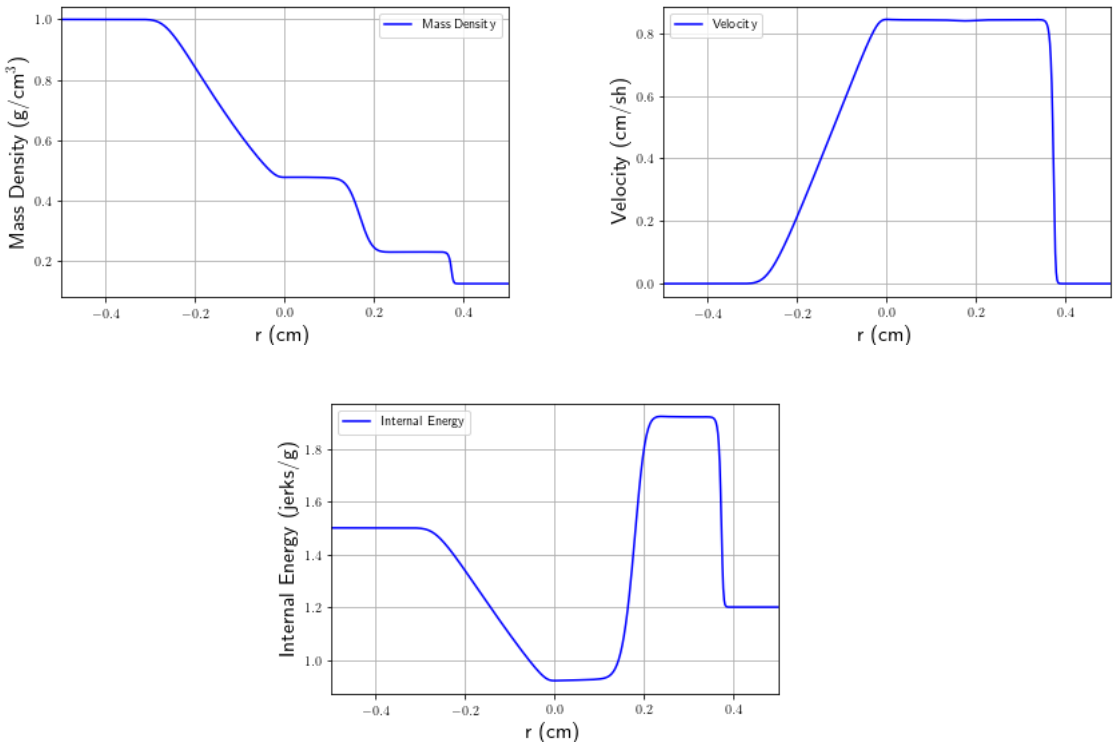

Figure 3: Shock tube problem results at $t = 0.2$ sh.

References

[1] Simon Bolding, Joshua Hansel, Jarrod D Edwards, Jim E Morel, and Robert B Lowrie. Second-order discretization in space and time for radiation-hydrodynamics. 338:511–526, 2017.

[2] Jarrod Edwards. The muscl-hancock method, April 2011.

[3] Ryan G McClarren and Robert B Lowrie. The effects of slope limiting on asymptotic-preserving numerical methods for hyperbolic conservation laws. *Journal of Computational Physics*, 227(23):9711–9726, 2008.

[4] Jim E. Morel. Nuen 627, radiation-hydrodynamics course notes.

[5] Eleuterio F Toro. *Riemann solvers and numerical methods for fluid dynamics: a practical introduction*. Springer Science & Business Media, 2013.